A SEMI-IMPLICIT METHOD FOR 3D FREE SURFACE FLOWS USING HIGH ORDER VELOCITY RECONSTRUCTION ON UNSTRUCTURED POLYGONAL VORONOI MESHES

Walter Boscheri, Michael Dumbser, Maurizio Righetti

[1]Department of Civil and Environmental Engineering, University of Trento, Italy, Via Mesiano, 77, I-38123 Trento
E-mail: walter.boscheri@unitn.it, michael.dumbser@unitn.it, maurizio.righetti@unitn.it

This paper presents an efficient *semi-implicit*numerical scheme for the solution of the *three-dimensional* incompressible Navier-Stokes equations, assuming a hydrostatic pressure distribution. For this equation system, in a series of papers, Casulli et al. (1992, 2000, 2011) have proposed a set of particularly efficient semi-implicit schemes both on structured and unstructured meshes. The method has subsequently been extended also to non-hydrostatic free surface flows, see Casulli et al. (2002). The most recent developments concern a rigorous, nonlinear and mass-conservative treatment of wetting and drying, presented by Casulli (2009), and an efficient use of subgrid resolution, see Casulli and Stelling (2011). In the above-mentioned articles, a semi-implicit approach is chosen in order to get stable schemes with large time steps at reasonable computational cost.

The semi-implicit method presented in this paper is implemented on general polygonal Voronoi meshes and follows the ideas of Casulli et al., i.e. the pressure terms are discretized *implicitly*, while the nonlinear convective terms are discretized *explicitly* using a semi-Lagrangian method, which is the only explicit method for the discretization of convective terms that allows for large time steps *without* imposing a CFL-type stability condition.The scheme uses a *staggered mesh* approach, i.e. the pressure is defined in the cell center, while the normal velocity componentsare saved on the element edges.This is common practice for the simulation of incompressible flows. The semi-Lagrangian method used for the nonlinear convective terms needs the integration backward in time along the trajectories of the fluid in order to find the foot of the characteristics.For that purpose, the *vector* velocity field has to be reconstructed from the known *scalar* normal velocity components at the element interfaces. Here, a *third order* polynomial reconstruction is used for the velocity. The reconstruction operator is based on integral conservation on element edges within a *stencil,* surrounding the control volume under consideration. To solve the resulting over-determined linear system of algebraic equations,a constrained least-squares formulation is used. The linear constraints may also contain a condition that the velocity field is divergence-free also on the discrete level. The concept of polynomial recovery from known cell averages has been introduced already by Barth and Frederickson (1990) and has been continuously developed since then in the context of high order *nonlinear* finite volume methods for systems of hyperbolic conservation laws.

Several academic test problems are presented to validate the proposed new scheme, however,even one realistic application is also considered, concerning a water supply channel of a small hydro-electric power plant, in order to show the potential of the algorithm for realistic 3D free surface flow applications with secondary flows.

The outline of this paper is as follows: first the governing PDE system is described, then the numerical method is analyzed, by presenting with more details the new high order velocity field reconstruction. Some academic test problems are performed, such as Blasius boundary layer theory and a stationary vortex flow. At the end of the paper it is shown an application of the new algorithm to an open channel flow, put to hydroelectric use.

Most state of the art free surface flow models commonly used in environmental engineering and geophysics are based on some kind of depth–averaged shallow water type flow model. The main drawback of this kind of model is the fact that the genuinely three-dimensional secondary circulations of flows in curved channels cannot be resolved. However, the flow may often be still considered hydrostatic. For this case, a new semi-implicit scheme is developed, which works on general unstructured polygonal meshes to resolve this kind of problem. The governing partial differential equations (PDE) are the three-dimensional incompressible Navier-Stokes equations with variable free surface η. Assuming a hydrostatic pressure, the governing PDE read as follows:

$$\frac{\partial u}{\partial t} + v \cdot \nabla u = -g \frac{\partial \eta}{\partial x} + \nabla \cdot (\nu \nabla u)$$
$$\frac{\partial v}{\partial t} + v \cdot \nabla v = -g \frac{\partial \eta}{\partial y} + \nabla \cdot (\nu \nabla v)$$
$$\nabla \cdot v = 0$$

$$\frac{\partial \eta}{\partial t} + \frac{\partial}{\partial x}\int_{-h}^{\eta} u\mathrm{d}z + \frac{\partial}{\partial y}\int_{-h}^{\eta} v\mathrm{d}z = 0 \tag{1}$$

In the above system, the first two equations derive from the momentum equations in the horizontal plane, the third equation is the divergence-free constraint on the velocity field and the last equation is the governing PDE for the free surface η.

The numerical scheme is based on a staggered-mesh approach, which is illustrated for the purpose of simplicity on a regular *two-dimensional*Cartesian grid in Figure 1 below. The horizontal velocity components *u* and *v,* as well as the vertical velocity component *w* are defined on the faces of a control volume $[x_{i-1/2};\ x_{i+1/2}]\mathrm{x}[y_{j-1/2};y_{j+1/2}]\mathrm{x}[z_{k-1/2};z_{k+1/2}]$, while the free surface η, equivalent to the pressure, is defined in the cell center (x_i,y_j,z_k).

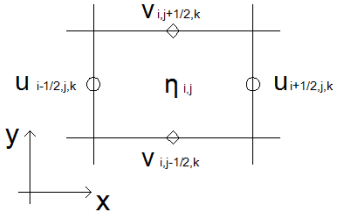

Figure 1:Staggered mesh on *x*-*y* plane with the free surface defined in the cell center and the velocities at the element boundaries.

An extension to general meshes is possible, however, in this case the grid must be constructed in such a way that it is at least *orthogonal*, i.e. the straight line connecting two pressure points across an element edge must be perpendicular to that edge. Such a mesh can be constructed using an underlying primary Delaunay triangulation and constructing successively the corresponding Voronoi mesh, whose control volumes are obtained by connecting for each node on the Delaunay mesh the *incircle* centers of each primary triangle adjacent to it.

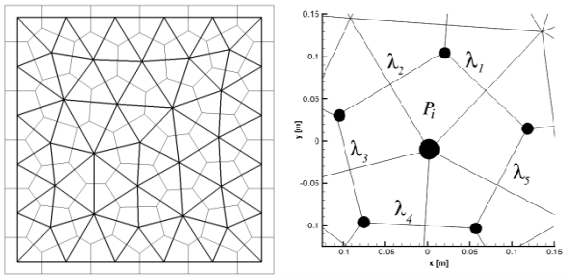

Figure 2:Primary triangular mesh and corresponding dual Voronoi mesh (left). Notation and zoom for an isolated polygonal Voronoi element (right).

A sketch of a primary mesh and the corresponding Voronoi mesh is given in Figure 2 on the left, while on the right of Figure 2 it is introduced the general notations used for the numerical scheme, hence P_i denotes the *i*-th polygon (control volume), and λj denotes the edge-length of each 2D control volume. In vertical *z* direction, the 2D elements are extruded, hence obtaining *prismatic* control volumes in 3D.

The discrete momentum equation reads

$$u_{j,k}^{n+1} = Fu_{j,k}^{n} - g\frac{\Delta t}{l_j}(\eta_R^{n+1} - \eta_L^{n+1}) + \frac{\nu \Delta t}{\Delta z_{j,k}^{n}}\left(\frac{\Delta u_{j,k+\frac{1}{2}}^{n+1}}{\Delta z_{j,k+\frac{1}{2}}^{n}} - \frac{\Delta u_{j,k-\frac{1}{2}}^{n+1}}{\Delta z_{j,k-\frac{1}{2}}^{n}}\right) \tag{2}$$

where $\Delta u_{j,k+\frac{1}{2}}^{n+1}=u_{j,k+1}^{n+1} - u_{j,k-1}^{n+1}$. Here, $u_{j,k}^{n}$ denotes the normal velocity component at edge *j* of the control volume at time level *n* on layer number *k* in vertical direction. $Fu_{j,k}^{n}$is defined in explicitly as the normal velocity at the *foot* of the characteristics, i.e. at the footpoint of the Lagrangian trajectory. The second term on the right hand side if (2) denotes the pressure gradient, where the indices *L* and *R* denote the left and right polygon adjacent to edge *j*, l_j is the distance between the left and right polygon, and the last term is the implicit discretization of the vertical viscosity. The discrete free surface equation reads

$$A_i\eta_i^{n+1} = A_i\eta_i^{n+1} - \frac{\Delta t}{A_i}\sum_{j=1}^{S_i}\left(s_{i,j}\lambda_j \sum_{k=m}^{M}\Delta z_{j,k}^{n}\mathrm{u}_{j,k}^{n+1}\right) \tag{3}$$

Here $s_{i,j}$ is the sign, which is +1 if the normal vector defined on edge *j* is outward-pointing with respect to polygon P_i and the sign is -1 if the normal vector is inward-pointing w.r.t. polygon P_i. Equation (2) can be formally substituted into eqn. (3), which then yields a symmetric positive definite linear algebraic equation system for the unknown free surface η. The system can be solved very efficiently with the conjugate gradient method. Once the new free surface location is known the normal velocities can be obtained from eqn. (2) and the vertical velocities *w* are obtained *a posteriori* from the following equation

$$w_{i,k+\frac{1}{2}}^{n+1} = w_{i,k-\frac{1}{2}}^{n+1} - \frac{1}{A_i}\sum_{j=1}^{S_i}\left(s_{i,j}\lambda_j\Delta z_{j,k}^{n}\mathrm{u}_{j,k}^{n+1}\right) \tag{4}$$

The main novelty of this paper consists in a high order polynomial velocity field reconstruction in order to compute the operator $Fu_{j,k}^n$, which is given by

$$Fu_{j,k}^n = v(x_j^L) \cdot n_j \tag{5}$$

where $n_j$is thenormal vector of edge number *j*,andx_j^Listhe foot of the Lagrangian trajectory, emerging in the center of edge jx_j.The foot of the trajectory is given by the solution $x_j^L = x(\Delta t)$of the following system of ordinary differential equations:

$$\frac{dx}{dt} = -v(x) \tag{6}$$

with the initial condition

$$x(0) = x_j \tag{7}$$

The trajectory is integrated using an explicit Taylor method, which up to second order reads as follows:

$$x^{m+1} = x^m - \Delta\tau v(x^m) + \frac{\Delta\tau}{2}\frac{\partial v}{\partial x}v(x^m) \tag{8}$$

where $\Delta\tau$ is a *local* time step that must obey a *local* Courant stability criterion. In equations (6) and (8) it has to be determined a *continuous* interpolation of the velocity field from the given normal velocity components at the element edges. For this purpose the yet unknown velocity field *v(x)*for each polygon $P_i$can be written as a high order polynomial using the Taylor series expanded about the polygon center x_i as

$$v(x) = \sum_{l=0}^{N-m}\sum_{m=0}^{N}\frac{(x-x_i)^l}{l!}\frac{(y-y_i)^m}{m!}\frac{\partial^{l+m}\boldsymbol{v}}{\partial x^l \partial y^m} \tag{9}$$

The unknown expansion coefficients in eqn. (9) are the derivatives of the velocity field. For a third degree polynomial, a total of 20 unknown coefficients are required, 10 for the *u* velocity component and 10 for the *v*velocity component. An equation system has to be assembled in order to determine them. The guideline here is integral conservation on all element edges *j* within a stencil S_i, which is an appropriate set of element edges surrounding polygon number *i*. For each vertical layer *k*is required that the integral average of the normal velocity of the polynomial (9) is identical to the known face normal velocity $u_{j,k}^n$.

$$\frac{1}{\lambda_j}\int_{\partial P_{ij}} v_k(x)\cdot n_j ds = u_{j,k}^n \quad \forall \partial P_{ij} \in S_i \tag{10}$$

Here, ∂P_{ij} denotes the edge *j* of polygon P_i. Equation (10) constitutes a linear algebraic equation system which is over determined, since *more* elements are needed than the necessary 20 elements, according to the findings of Barth and Frederickson (1990), who were the first authors to propose a better than second order accurate finite volume scheme on general unstructured triangular meshes. Relation (10) must hold exactly at least for all edges of polygon P_i itself, hence the system (10) is solved using a *constrained* least-squares method, where the linear constraint is enforced using a Lagrangian multiplier method, see Dumbser et al. (2007) for details. A similar approach is also used for the vertical velocity component *w*. In vertical *z* direction, the resulting polynomial is obtained via classical Lagrange interpolation. This completes the description of the numerical method.

Now some computational results on academic tests are presented and finally an application to a realistic world problem is also performed. All measurements and quantities are expressed by adopting the International System of Units.

1. Circular Planar Trajectories

The first test considers the reconstruction of a circular trajectory from a velocity field given by a rigid body rotation as

$$v(x) = \Omega \times x \tag{11}$$

The trajectories are closed circles and the period of rotation is given by the angular frequency $\boldsymbol{\Omega}$= (0,0,1) for a rotation in the *x*-*y* plane and by $\boldsymbol{\Omega}$= (0,1,0) for a rotation in the *x*-*z* plane, respectively. The solutions of the integrated trajectories starting in one representative point are depicted for both cases in Figure 3. It can be noticed an excellent agreement between the exact and the numerical solution.

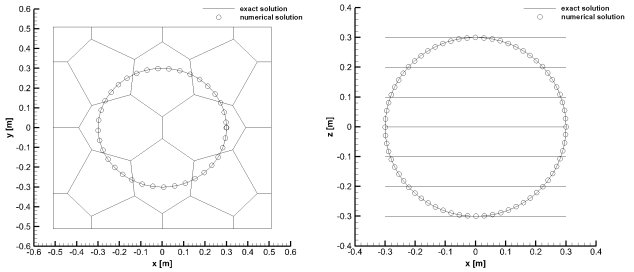

Figure 3: Circular planar trajectory in the *x*-*y* plane (left) and circular planar trajectory in the *x*-*z* plane (right). The symbols represent the numerical solution, the solid line is the exact solution for the trajectory.

2. Laminar Boundary Layer Flow

In this section a laminar stationary boundary layer flow problem over a flat plate is solved. The plate has length L=1, the inflow velocity is v = (1,0,0), and the kinematic viscosity of the fluid is $\nu = 10^{-4}$. Although the resulting Reynolds number is unphysically high for a laminar boundary layer, it is nevertheless a very useful test problem to validate numerical algorithms. The comparison between the exact Blasius solution, see Schlichting and Gersten (2005), and the numerical results depicted in Figure 4 is very satisfactory.

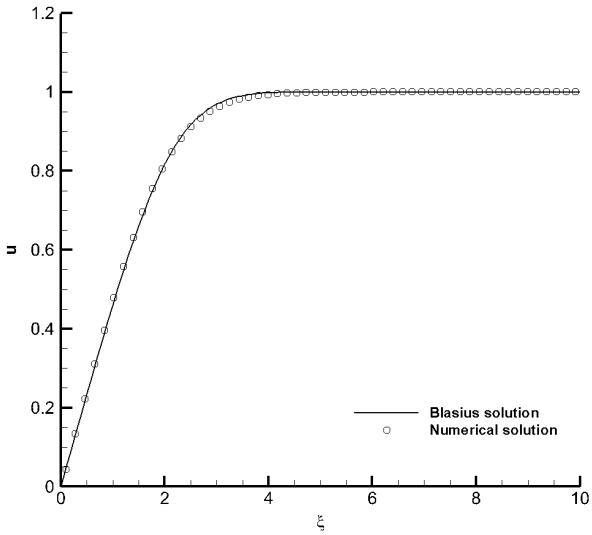

Figure 4: Numerical and exact solution for the laminar Blasius boundary layer developing on a flat plate. The velocity profile *u(y)* is taken at ξ=0.9 and the results are depicted in dimensionless coordinates, see Schlichting and Gersten (2005).

3. Stationary vortex

In this test problem a stationary vortex flow with variable free surface is considered. The viscous terms are neglected here so that the motion of the fluid is governed by a perfect balance between the pressure gradient and thecentrifugalforce. Theradialmomentumbalancereads

$$\frac{\partial \eta}{\partial r} = \frac{u_\phi^2}{gr} \tag{12}$$

where r is the radial coordinate and uφ is the angular velocity. Here, the following choice is madefor the angular velocity:

$$u_\phi = rexp\left(-\frac{1}{2}(r^2 - 1)\right) \tag{13}$$

The primary horizontal domain Ω_{xy}^p is a circle with diameter d=*10* and the free surface is given by integration of eqn(12) using eqn.(13)

$$\eta(r) = \int \frac{u_\phi^2}{gr} dr = \eta_\infty - \frac{1}{2g} \exp\,(1 - r^2) \tag{14}$$

with the integration constant $\eta_\infty \coloneqq 1$. Figure 5 shows the chosen initial condition for the angular velocity and for the free surface.

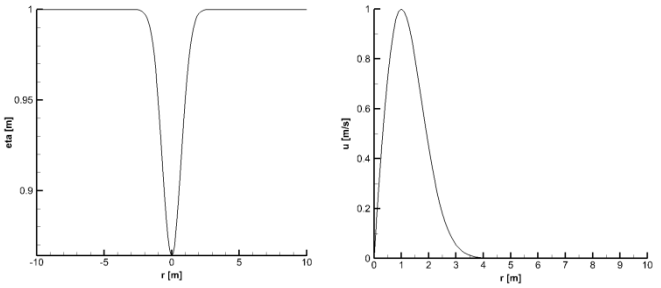

Figure 5: Initial condition for the free surface, on the left, and for the angular velocity, on the right.

Equations (13) and (14) describe the exact solution of a steady flow, where pressure force and centrifugal force are in perfect balance. The result are depicted in Figure 6 at an output time *t=0.5*. It can be noticed that the choice of the time step has an important influence on the accuracy of the results, which is due to the use of an Eulerian-Lagrangian scheme for the discretization of the nonlinear convective terms.

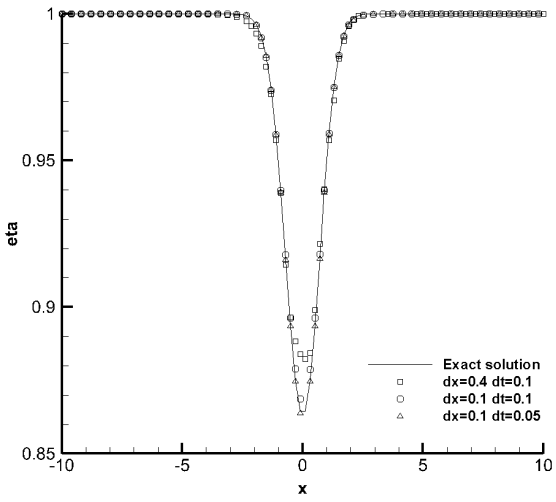

Figure 6: Results for the vortex test: difference results are obtained by performing different choices on either space step or time step.

4. *Application to a realistic case*

The algorithm has also applied to a realistic open flow channel: the channel of Maleo, which starts from its main river called *Adda* and is an open flow channel in the Lombardia region in Italy, closed to the town of Maleo.

Figure 7: The curved channel of Maleo with the bridge pier.

It's a derivation channel used to supply a small hydroelectric power plant. The engine room is equipped with two Kaplan turbines and is located at the end of the channel. At the beginning of the channel there is a bridge pier, which dissipates energy by creating a hydraulic jump. The main problem is given by a left bend in the channel's geometry, which causes three-dimensional secondary circulations, so that there is a different flow rate between the external and the internal turbine. This problem prevents to achieve optimal efficiency, thus wasting hydroelectric energy and decreasing profits. The operator of the power plant requested some numerical simulations to understand the flow physics and to propose some possible solution strategies. For that purpose, it is possible to use the hydrostatic three-dimensional semi-implicit model presented in this paper.

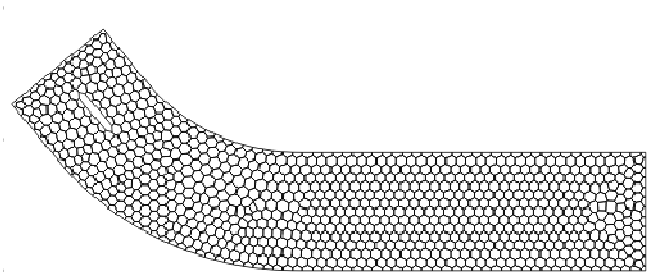

Figure 8: Unstructured polygonal Voronoi mesh used to discretize the *x*-*y* plane of the Maleo channel. On the left the bridge pier can be noted.

A photograph of the channel under consideration is shown in Figure 7 and a two-dimensional sketch of the unstructured Voronoi mesh used is depicted in Figure 8. It has to be consider that the real mesh is three dimensional due to the use of prismatic elements, simply obtained by extruding the 2D element in vertical direction.

The computational results are depicted in the following. Figure 9 shows the depth-averaged velocity distribution in the *x*-*y* plane and Figure 10 shows a cut through the *y*-*z* plane, visualizing the secondary flows. With the new numerical simulations it was possible to confirm that the interior turbine gets about 20% less mass flow than the exterior turbine, which was also found in field measurements.

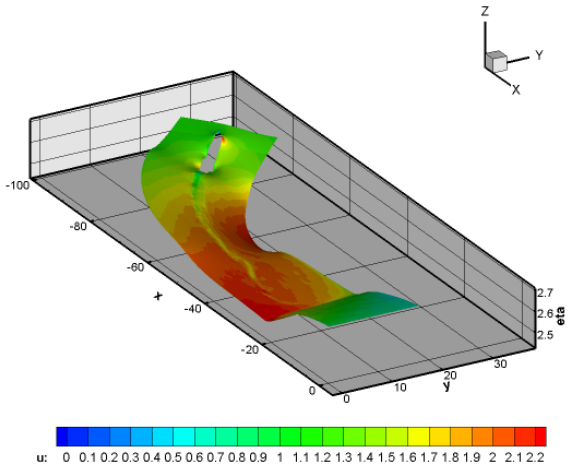

Figure 9: Depth-averaged velocity distribution in *m/s*.

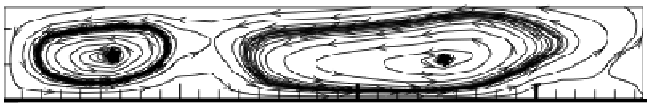

Figure 10: Secondary flows in the *y*-*z* plane at $x = -25$.

Conclusions

In this article an efficient semi-implicit scheme for the simulation of three-dimensional hydrostatic free surface flows has been implemented on staggered polygonal Voronoi meshes. The pressure terms are discretized implicitly while the convective terms are discretized with an explicit semi-Lagrangian schemes, which needs the integration of Lagrangian trajectories. For that purpose a high order velocity field reconstruction operator has been presented. The resulting scheme has been carefully validated on a suite of test problems with exact solution and finally on a realistic channel. Future work may concern the

extension to realistic turbulence models and bed-load transport.

References

[1] V. Casulli and R. Cheng (1992). Semi-implicit finite difference methods for three–dimensional shallow water flow. *International Journal for Numerical Methods in Fluids*,**15**:629–648.

[2] V. Casulli and R. Walters (2000). An unstructured grid, three–dimensional model based on the shallow water equations. *International Journal for Numerical Methods in Fluids*; **32**:331–348.

[3] V. Casulli (2009). A high-resolution wetting and drying algorithm for free surface hydrodynamics. *International Journal for Numerical Methods in Fluids*, **60**:391–408.

[4] V. Casulli and G. Stelling (2011). Semi-implicit subgridmodelling of three-dimensional free-surface flows. *International Journal for Numerical Methods in Fluids*, **67**:441–449.

[5] V. Casulli and P. Zanolli (2002). Semi-implicit numerical modeling of nonhydrostatic free-surface flows for environmental problems. *Mathematical and Computer Modelling*; **36**:1113–1149.

[6] T. Barth and P. Frederickson (1990). Higher order solution of the Euler equations on unstructured grids using quadratic reconstruction. *AIAA paper no. 90-0013* 28th Aerospace Sciences Meeting January 1990.

[7] H. Schlichting, K. Gersten (2005). *Grenzschicht-Theorie*. Springer Verlag Berlin-Heidelberg.

[8] M. Dumbser and M. Käser (2007). Arbitrary High Order Non-Oscillatory Finite Volume Schemes on Unstructured Meshes for Linear Hyperbolic Systems, *Journal of Computational Physics*, **221**:693-723.